Electronic Supplementary Material (ESI) for Physical Chemistry Chemical Physics.

Supporting Information

Light-induced charge separation process in P3HT/$PC_{70}BM$ composite as studied by out-of-phase electron spin echo spectroscopy

*Ekaterina A. Lukina[1,2], Alexander A. Popov[1,2], Mikhail N. Uvarov[1], Elizaveta A. Suturina[2,3],Edward J. Reijerse[3], Leonid V. Kulik[1,2]**

[1] Voevodsky Institute of Chemical Kinetics and Combustion of Siberian Branch of Russian Academy of Sciences, Institutskaya 3, 630090 Novosibirsk, Russia

[2] Novosibirsk State University, Pirogova 2, 630090 Novosibirsk, Russia

[3] Max Planck Institute for Chemical Energy Conversion, Stiftstrasse 34-36, D-45470 Mulheim an der Ruhr, Germany

Theory

Analytical calculation of echo intensity

We calculated echo shape and intensity for two-pulse microwave sequence with a non-ideal first pulse (duration t_p, nominal flip angle α, see Scheme 1 in the main text) for two-spin system.

The spin-hamiltonian of the radical pair comprises Zeeman interactions of both spins with the external magnetic field and the magnetic interaction between the spins in the radical pair (Eq. 1 of the main text), $\hat{H} = \omega_1 \hat{S}_{1z} + \omega_2 \hat{S}_{2z} + \Gamma \hat{S}_{1z} \hat{S}_{2z}$. During the first pulse we can neglect the interaction between two spins, since $t_p \Gamma << 1$. In this case we can rewrite spin-hamiltonian as

$$\hat{H} = \gamma(\hat{S}_1, B_{eff\,(1)}) + \gamma(\hat{S}_2, B_{eff\,(2)}),$$

where $B_{\mathrm{eff(i)}}=(B_1,0,B_0-\omega_0/g_i\beta)$ are effective magnetic field for the spin i, i = 1, 2. Therefore, during the action of microwave pulse evolution of spins 1 and 2 can be treated separately and simple vector model can be applied. For this reason the action of the non-ideal pulse was modeled as a rotation of the vector of individual spins around the corresponding effective magnetic field $B_{\mathrm{eff(i)}}$. Since resonance positions are different for the two spins the effective angles of rotation $\alpha_i = \alpha|\ B_{\mathrm{eff(i)}}|/B_1$ are also different. The matrix representing the rotation around $B_{\mathrm{eff(i)}}$ by angle α_i was calculated as $P_\mathrm{i}'=P_\mathrm{i}''P_\mathrm{i}P_\mathrm{i}''^{\mathrm{T}}$, where

$P_i = \begin{bmatrix} 1 & 0 & 0 \\ 0 & \cos\alpha_i & \sin\alpha_i \\ 0 & -\sin\alpha_i & \cos\alpha_i \end{bmatrix}$ is the rotation of magnetization vector around B_1 by angle α_i and

$P_i'' = \begin{bmatrix} \sin\varphi_i & 0 & -\cos\varphi_i \\ 0 & 1 & 0 \\ \cos\varphi_i & 0 & \sin\varphi_i \end{bmatrix}$ is the rotation around the axis y by angle $\pi/2-\varphi_\mathrm{i}$, so that after this rotation direction of B_1 turns into the direction of B_{eff}. Here φ_i is the angle between $B_{\mathrm{eff(i)}}$ and B_0;

$\sin\varphi_i = \dfrac{B_1}{\left(B_0 - \omega_0/g_i\beta\right)^2 + B_1^2}$ and $\cos\varphi_i = \dfrac{B_0 - \omega_0/g_i\beta}{\left(B_0 - \omega_0/g_i\beta\right)^2 + B_1^2}$.

Thus we obtained the transformation matrix for rotation of individual spins by non-ideal pulse

$$P_i' = \begin{bmatrix} \cos^2\phi_i\cos\alpha_i + \sin^2\phi_i & \cos\phi_i\sin\alpha_i & \sin\phi_i\cos\phi_i\left(1-\cos\alpha_i\right) \\ -\cos\phi_i\sin\alpha_i & \cos\alpha_i & \sin\phi_i\sin\alpha_i \\ \sin\phi_i\cos\phi_i\left(1-\cos\alpha_i\right) & -\sin\phi_i\sin\alpha_i & \sin^2\phi_i\cos\alpha_i + \cos^2\phi_i \end{bmatrix}.$$

The period of free evolution during time τ with Hamiltonian $H = \omega_1 S_{1z} + \omega_2 S_{2z} + \Gamma S_{1z} S_{2z}$ was calculated using conventional product-operator formalism. The second microwave pulse was considered as ideal and therefore the evolution of the magnetization was determined by operator $\omega_1\tau S_{1z} + \omega_2\tau S_{2z}$. The second period of free evolution during $\tau+t$ was calculated the same way as a first one. The result of the calculation was averaged over $\omega_1\tau$ and $\omega_2\tau$ to take into account inhomogeneous broadening of EPR lines. Only the terms that result in the observable components of the magnitude were maintained during the calculation.

Using this procedure we performed the following calculation for the initial density matrix $\rho_0^{net(1)} = S_{1z}$, corresponding to net polarization of the spin 1. Since

$$\begin{bmatrix} \cos^2\varphi_1\cos\alpha_1 + \sin^2\varphi_1 & \cos\varphi_1\sin\alpha_1 & \sin\varphi_1\cos\varphi_1(1-\cos\alpha_1) \\ -\cos\varphi_1\sin\alpha_1 & \cos\alpha_1 & \sin\varphi_1\sin\alpha_1 \\ \sin\varphi_1\cos\varphi_1(1-\cos\alpha_1) & -\sin\varphi_1\sin\alpha_1 & \sin^2\varphi_1\cos\alpha_1 + \cos^2\varphi_1 \end{bmatrix} \begin{bmatrix} 0 \\ 0 \\ 1 \end{bmatrix} = \begin{bmatrix} \sin\varphi_1\cos\varphi_1(1-\cos\alpha_1) \\ -\sin\varphi_1\sin\alpha_1 \\ \sin^2\varphi_1\cos\alpha_1 + \cos^2\varphi_1 \end{bmatrix},$$

after the first non-ideal microwave pulse we obtained:

$$\rho_1^{net(1)} = S_{1x}\sin\varphi_1\cos\varphi_1(1-\cos\alpha_1) - S_{1y}\sin\varphi_1\sin\alpha_1 + S_{1z}(\sin^2\varphi_1\cos\alpha_1 + \cos^2\varphi_1)$$

The term proportional to S_{1z} was further omitted because it does not result in the observable magnetization at the echo detection moment.

After the period τ of free evolution the density matrix becomes

$$\rho_2^{net(1)} = \left[\left(S_{1x}\cos\Gamma\tau/2 + 2S_{1y}S_{2z}\sin\Gamma\tau/2\right)\cos\omega_1\tau + \left(S_{1y}\cos\Gamma\tau/2 - 2S_{1x}S_{2z}\sin\Gamma\tau/2\right)\sin\omega_1\tau\right]\sin\varphi_1\cos\varphi_1(1-\cos\alpha_1) -$$
$$-\left[\left(S_{1y}\cos\Gamma\tau/2 - 2S_{1x}S_{2z}\sin\Gamma\tau/2\right)\cos\omega_1\tau - \left(S_{1x}\cos\Gamma\tau/2 + 2S_{1y}S_{2z}\sin\Gamma\tau/2\right)\sin\omega_1\tau\right]\sin\varphi_1\sin\alpha_1$$

Ideal π-pulse inverts the magnetization with respect to x axis and we obtain

$$\rho_3^{net(1)} = \left[\left(S_{1x}\cos\Gamma\tau/2 - 2S_{1y}S_{2z}\sin\Gamma\tau/2\right)\cos\omega_1\tau + \left(-S_{1y}\cos\Gamma\tau/2 - 2S_{1x}S_{2z}\sin\Gamma\tau/2\right)\sin\omega_1\tau\right]\sin\varphi_1\cos\varphi_1(1-\cos\alpha_1) -$$
$$-\left[\left(-S_{1y}\cos\Gamma\tau/2 - 2S_{1x}S_{2z}\sin\Gamma\tau/2\right)\cos\omega_1\tau - \left(S_{1x}\cos\Gamma\tau/2 - 2S_{1y}S_{2z}\sin\Gamma\tau/2\right)\sin\omega_1\tau\right]\sin\varphi_1\sin\alpha_1$$

After the second period of free evolution $\tau+t$ we obtain the following in-phase and out-of-phase components of the magnetization.

$$S_y^{net(1)}(\tau,t) \propto \sin\varphi_1\cos\varphi_1(1-\cos\alpha_1)\left[\sin\omega_1 t\cos\Gamma t/2\cos\Gamma\tau - \sin\omega_1 t\sin\Gamma t/2\sin\Gamma\tau\right] -$$
$$-\sin\varphi_1\sin\alpha_1\left[\cos\omega_1 t\sin\Gamma t/2\sin\Gamma\tau - \cos\omega_1 t\cos\Gamma t/2\cos\Gamma\tau\right]$$

$$S_x^{net(1)}(\tau,t) \propto \sin\varphi_1\cos\varphi_1(1-\cos\alpha_1)\left[\cos\omega_1 t\cos\Gamma t/2\cos\Gamma\tau - \cos\omega_1 t\sin\Gamma t/2\sin\Gamma\tau\right] -$$
$$-\sin\varphi_1\sin\alpha_1\left[\sin\omega_1 t\sin\Gamma t/2\sin\Gamma\tau + \sin\omega_1 t\cos\Gamma t/2\cos\Gamma\tau\right]$$

At the moment t=0 (the central position of the echo in time domain) these expressions are simplified:

$$S_y^{net(1)}(\tau) \propto \sin\varphi_1 \sin\alpha_1 \cos\Gamma\tau \quad \text{(S1)}$$

$$S_x^{net(1)}(\tau) \propto \sin\varphi_1 \cos\varphi_1 (1-\cos\alpha_1)\cos\Gamma\tau \,. \quad \text{(S2)}$$

The analogous results for initial net polarization of the second spin can be obtained from Eqs. S1, S2 by simple change of index i from 1 to 2. These equations can be used for isolated spins; for this case $\Gamma = 0$ should be used. Eq. S2 shows that for non-ideal microwave pulse out-of-phase echo appears even if electron spin in the radical pair is not correlated, but have some net polarization. For completely nonselective (ideal) microwave pulse $\sin\varphi_i = 1$, $\cos\varphi_i = 0$, so out-of-phase echo vanishes, as expected.

The analogous calculation was done for the initial density matrix representing spin-correlated radical pair in the singlet state (with zero- and double quantum coherences averaged out) $\rho_0^{SCRP}=S_{1z}S_{2z}$. Again only the terms resulting in the observable magnetization are kept.

Using the vector model-based approach similar to that described above we obtained after the first non-ideal microwave pulse:

$$\rho_1^{SCRP} = S_{1x}S_{2z}\sin\varphi_1\cos\varphi_1(1-\cos\alpha_1)\left(\sin^2\varphi_2\cos\alpha_2+\cos^2\varphi_2\right)+S_{1y}S_{2z}\sin\varphi_1\sin\alpha_1\left(\sin^2\varphi_2\cos\alpha_2+\cos^2\varphi_2\right)+$$
$$+S_{1z}S_{2x}\left(\sin^2\varphi_1\cos\alpha_1+\cos^2\varphi_1\right)\sin\varphi_2\cos\varphi_2(1-\cos\alpha_2)+S_{1z}S_{2y}\left(\sin^2\varphi_1\cos\alpha_1+\cos^2\varphi_1\right)\sin\varphi_2\sin\alpha_2$$

After the period τ of free evolution the terms $S_{1x}S_{2z}$ and $S_{1y}S_{2z}$ become

$$S_{1x}S_{2z} \to \left(2S_{1x}S_{2z}\cos\Gamma\tau/2+S_{1y}\sin\Gamma\tau/2\right)\cos\omega_1\tau+\left(2S_{1y}S_{2z}\cos\Gamma\tau/2-S_{1x}\sin\Gamma\tau/2\right)\sin\omega_1\tau \text{ and}$$

$$S_{1y}S_{2z} \to \left(2S_{1y}S_{2z}\cos\Gamma\tau/2-S_{1x}\sin\Gamma\tau/2\right)\cos\omega_1\tau-\left(2S_{1y}S_{2z}\cos\Gamma\tau/2+S_{1y}\sin\Gamma\tau/2\right)\sin\omega_1\tau \text{, respectively.}$$

Similar expressions for $S_{1z}S_{2x}$ and $S_{1z}S_{2y}$ can be written by interchange of indexes 1 and 2 in the expressions for $S_{1x}S_{2z}$ and $S_{1y}S_{2z}$.

After the π pulse and second period of free evolution τ+t the following in-phase and out-of-phase observable components of the magnetization. Also we averaged the signal over $\omega_1\tau$ and $\omega_2\tau$.

$$S_y^{SCRP}(\tau,t) \propto \sin\varphi_1\cos\varphi_1(1-\cos\alpha_1)\left(\sin^2\varphi_2\cos\alpha_2+\cos^2\varphi_2\right)\left[\cos\omega_1 t\sin\Gamma t/2\cos\Gamma\tau+\cos\omega_1 t\cos\Gamma t/2\sin\Gamma\tau\right]+$$
$$+\sin\varphi_2\cos\varphi_2(1-\cos\alpha_2)\left(\sin^2\varphi_1\cos\alpha_1+\cos^2\varphi_1\right)\left[\cos\omega_2 t\sin\Gamma t/2\cos\Gamma\tau+\cos\omega_2 t\cos\Gamma t/2\sin\Gamma\tau\right]+$$
$$+\sin\varphi_1\sin\alpha_1\left(\sin^2\varphi_2\cos\alpha_2+\cos^2\varphi_2\right)\left[\sin\omega_1 t\sin\Gamma t/2\cos\Gamma\tau+\sin\omega_1 t\cos\Gamma t/2\sin\Gamma\tau\right]+$$
$$+\sin\varphi_2\sin\alpha_2\left(\sin^2\varphi_1\cos\alpha_1+\cos^2\varphi_1\right)\left[\sin\omega_2 t\sin\Gamma t/2\cos\Gamma\tau+\sin\omega_2 t\cos\Gamma t/2\sin\Gamma\tau\right]$$

$$S_x^{SCRP}(\tau,t) \propto \sin\varphi_1\cos\varphi_1(1-\cos\alpha_1)\left(\sin^2\varphi_2\cos\alpha_2+\cos^2\varphi_2\right)\left[\sin\omega_1 t\sin\Gamma t/2\cos\Gamma\tau+\sin\omega_1 t\cos\Gamma t/2\sin\Gamma\tau\right]+$$
$$+\sin\varphi_2\cos\varphi_2(1-\cos\alpha_2)\left(\sin^2\varphi_1\cos\alpha_1+\cos^2\varphi_1\right)\left[\sin\omega_2 t\sin\Gamma t/2\cos\Gamma\tau+\sin\omega_2 t\cos\Gamma t/2\sin\Gamma\tau\right]+$$
$$+\sin\varphi_1\sin\alpha_1\left(\sin^2\varphi_2\cos\alpha_2+\cos^2\varphi_2\right)\left[\cos\omega_1 t\cos\Gamma t/2\sin\Gamma\tau+\cos\omega_1 t\sin\Gamma t/2\cos\Gamma\tau\right]+$$
$$+\sin\varphi_2\sin\alpha_2\left(\sin^2\varphi_1\cos\alpha_1+\cos^2\varphi_1\right)\left[\cos\omega_2 t\cos\Gamma t/2\sin\Gamma\tau+\cos\omega_2 t\sin\Gamma t/2\cos\Gamma\tau\right]$$

At the moment t=0 these expressions become

$$S_y^{SCRP}(\tau) \propto \left[\begin{array}{l}\sin\varphi_1\cos\varphi_1(1-\cos\alpha_1)\left(\sin^2\varphi_2\cos\alpha_2+\cos^2\varphi_2\right)+\\ \sin\varphi_2\cos\varphi_2(1-\cos\alpha_2)\left(\sin^2\varphi_1\cos\alpha_1+\cos^2\varphi_1\right)\end{array}\right]\sin\Gamma\tau \qquad \text{(S3)}$$

$$S_x^{SCRP}(\tau) \propto \left[\sin\varphi_1\sin\alpha_1\left(\sin^2\varphi_2\cos\alpha_2+\cos^2\varphi_2\right)+\sin\varphi_2\sin\alpha_2\left(\sin^2\varphi_1\cos\alpha_1+\cos^2\varphi_1\right)\right]\sin\Gamma\tau \qquad \text{(S4)}$$

As can be noticed from these equations, in-phase ESEEM appears for SCPR if microwave pulse is non-ideal. For the case of nonselective pulses it becomes zero, in accordance with previous theoretical results.

Figures

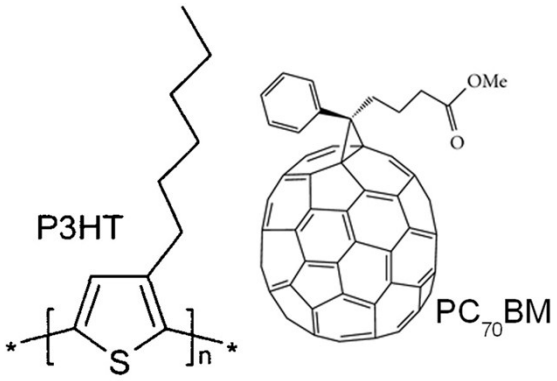

Figure S1. Molecular structures of poly(3-hexylthiophene) (P3HT) and [6,6]-phenyl-C71-butyric acid methyl ester ($PC_{70}BM$).

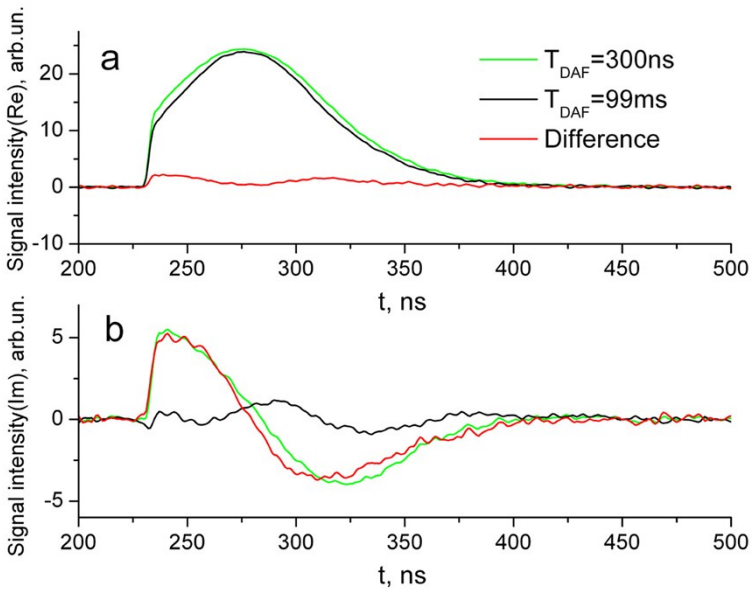

Figure S2. In-phase (a) and out-of-phase (b) echo shape of P3HT/$PC_{70}BM$ measured at 65 K with T_{DAF} 300ns and 99 ms and their difference (green, black and red lines respectively). The two-pulse microwave sequence with nonselective pulses and τ = 120 ns was used. Measurements were done in the maximum of the out-of-phase signal (g=2.0033).

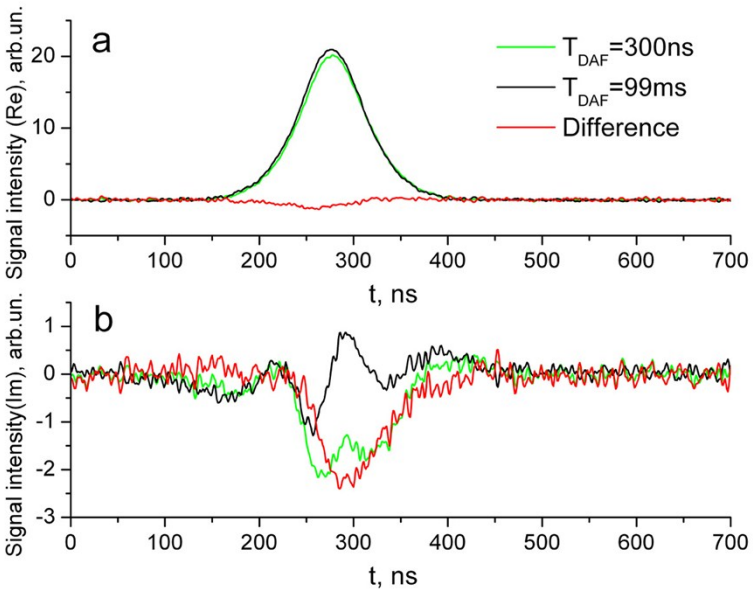

Figure S3. In-phase (a) and out-of-phase (b) echo shape of P3HT/$PC_{70}BM$ measured at 65 K with T_{DAF} 300ns and 99 ms and their difference (green, black and red lines respectively). The two-pulse microwave sequence with nonselective pulses and τ = 400 ns was used. Measurements were done in the maximum of the out-of-phase signal (g=2.0033).

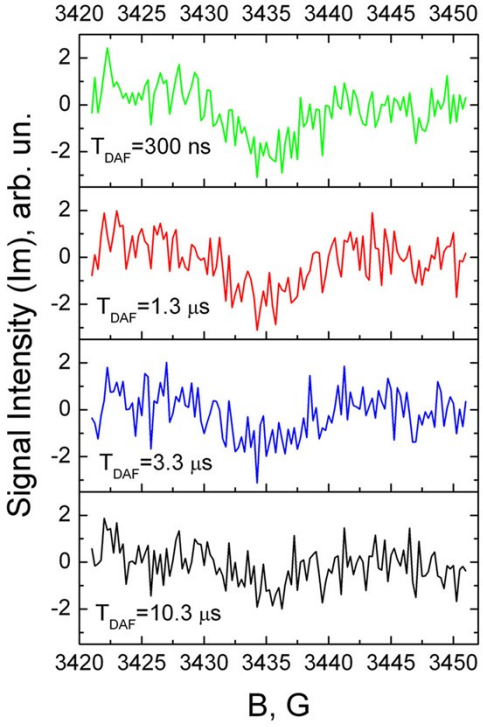

Figure S4. Out-of-phase echo detected EPR spectra of P3HT/$PC_{70}BM$ evolution with increasing delay between laser flash and microwave pulse sequence. Temperature 65 K. The flash-induced signals were obtained by subtraction of the background signal with T_{DAF}=99ms from signals with indicated T_{DAF}. The two-pulse microwave sequence with nonselective pulses and τ = 400 ns was used.

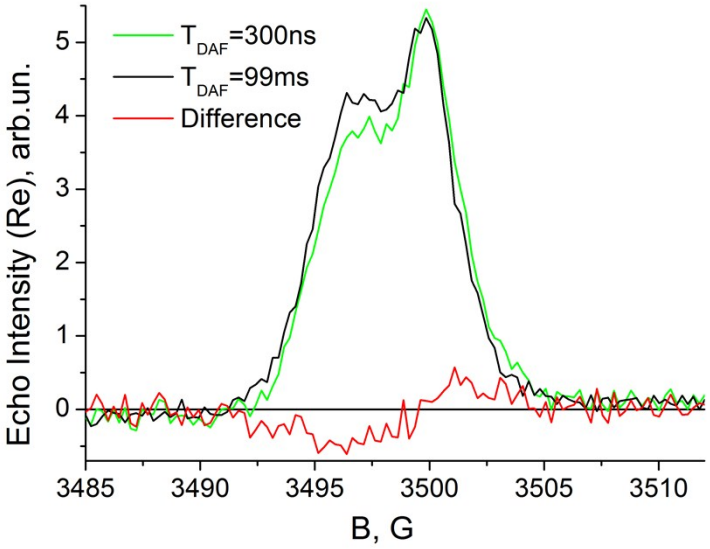

Figure S5. In-phase echo detected EPR spectrum of P3HT/$PC_{70}BM$ measured at 65 K with T_{DAF}=300 ns and 99 ms and flash-induced signal determined as their difference (green, black and red lines respectively). The two-pulse microwave sequence with selective pulses 100ns - τ = 400ns - 200ns was used.

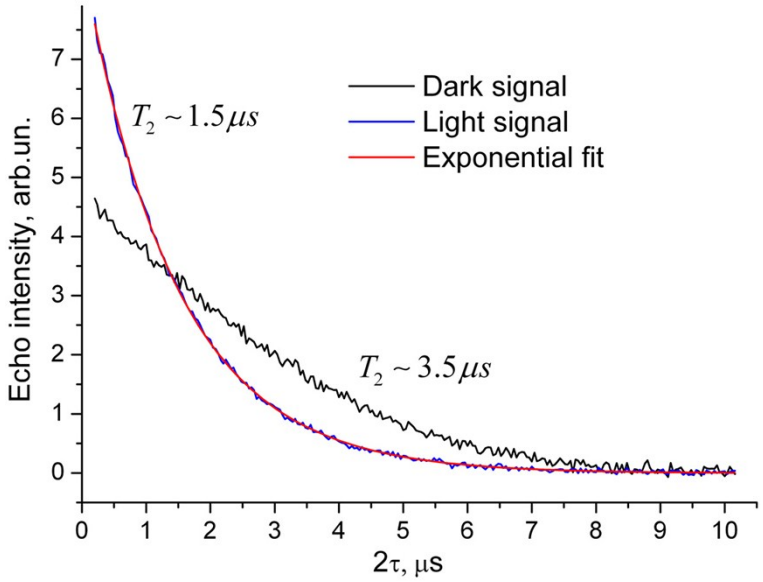

Figure S6. Signal decay (Re) with increasing delay τ between the microwave pulses measured at 65 K at the point of maximum in-phase signal intensity (g=2.0036). Black line represents the dark signal with a characteristic decay time 3.5 μs; the blue line represents the signal under continuous light illumination, fitted by exponential decay (red line) with decay time 1.5 μs.

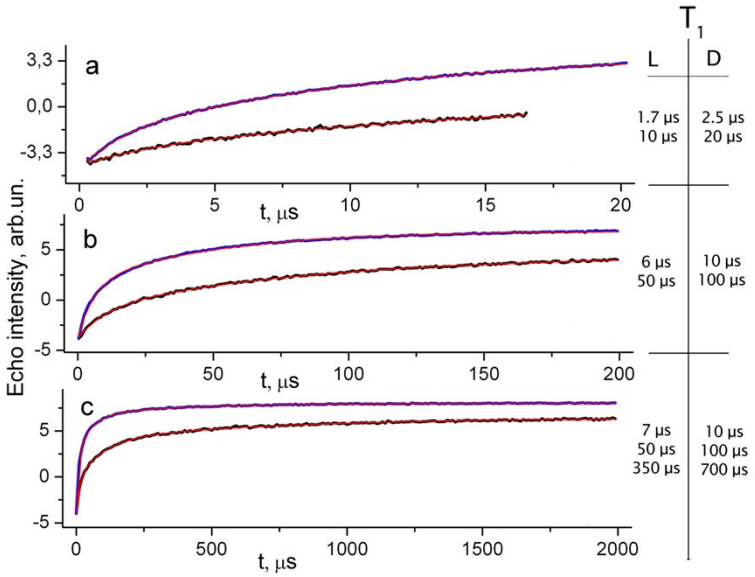

Figure S7. Signal decay (Re) with increasing delay T in inversion-recovery microwave pulse sequence π-T-π/2-τ-π measured at 65 K at the point of maximum in-phase signal intensity

(g=2.0036). Black line represents dark signal; blue one – signal under continuous light illumination. All signals were fitted by two or three exponential decays (red line). Characteristic T_1 times of light and dark signals for each time scale are shown.

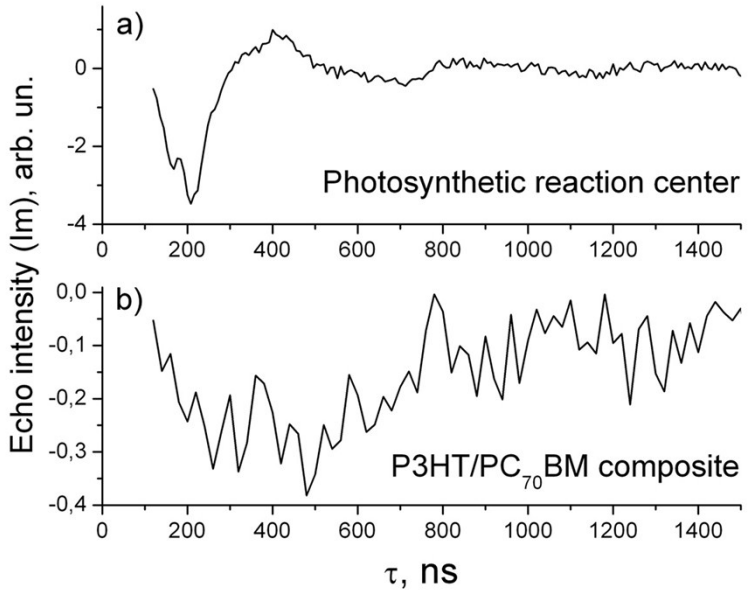

Figure S8. Out-of-phase ESEEM recorded at 65 K, T_{DAF}=300ns. a) signal of Zn-substituted *Rhodobacter sphaeroides* R26 photosynthetic reaction center measured in the maximum of the out-of-phase signal (g=2.0045). b) field-averaged signal in P3HT/PC_{70}BM composite.

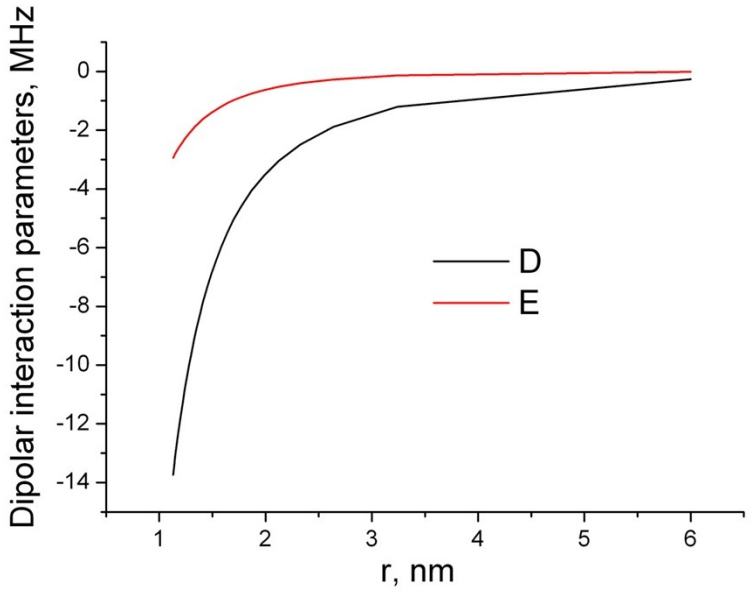

Figure S9. Zero-field splitting parameters *D* and *E* of the triplet state of fullerene$^-$/polythiophene$^+$ (18 unit chain) calculated by means of DFT as a function of distance between their centers.

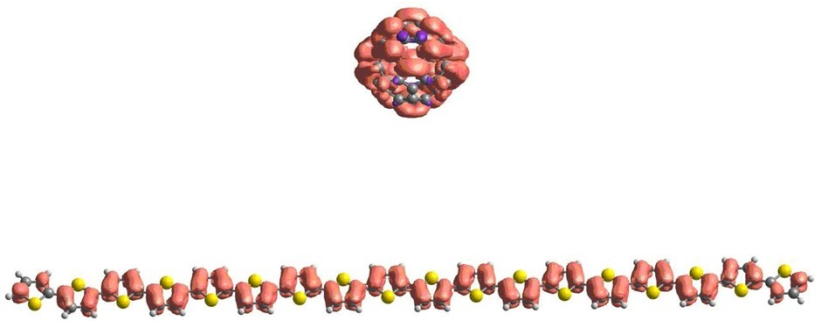

Figure S10. Electron spin density on fullerene$^-$/polythiophene$^+$ calculated by quantum chemistry. The distance between the center of fullerene molecule and polymer chain is 3 nm. Contour value is 0.0003.